

An Effective Action for Finite Temperature Lattice Gauge Theories with Dynamical Fermions

Peter N. Meisinger and Michael C. Ogilvie

Department of Physics, Washington University, St. Louis, MO 63130

(November 20, 2018)

Abstract

Dynamical fermions induce via the fermion determinant a gauge-invariant effective action. In principle, this effective action can be added to the usual gauge action in simulations, reproducing the effects of closed fermion loops. Using lattice perturbation theory at finite temperature, we compute for staggered fermions the one-loop fermionic corrections to the spatial and temporal plaquette couplings as well as the leading Z_N symmetry breaking coupling. A. Hasenfratz and T. DeGrand have shown that β_c for dynamical staggered fermions can be accurately estimated by the formula $\beta_c = \beta_c^{\text{pure}} - \Delta\beta_F$ where $\Delta\beta_F$ is the shift induced by the fermions at zero temperature. Numerical and analytical results indicate that the finite temperature corrections to the zero-temperature calculation of A. Hasenfratz and T. DeGrand are small for small values of $\kappa = \frac{1}{2m_F}$, but become significant for intermediate values of κ . The effect of these finite temperature corrections is to ruin the agreement of the Hasenfratz-DeGrand calculation with Monte Carlo data. We argue, however, that the finite temperature corrections are suppressed nonperturbatively at low temperatures, resolving this apparent disagreement. The Z_N symmetry breaking coupling is small; we argue that it changes the order of the transition

while having little effect on the critical value of β .

PACS number(s): 12.38.G, 12.38.Mh, 11.10.Wx

I. INTRODUCTION

It has been known for some time that the effects of heavy dynamical fermions can be included in Monte Carlo simulations by a hopping parameter expansion of the fermion determinant. This is reminiscent of the Euler-Heisenberg Lagrangian of perturbative QED, in which the effects of electron loops are included in a gauge-invariant effective Lagrangian. Recently Hasenfratz and DeGrand [1,2] have performed a zero-temperature calculation of the shift in the lattice gauge coupling constant β , defined as $\beta = 2N_c/g^2$, induced by staggered dynamical fermions and applied the result to the finite temperature phase transition in QCD. Their result for the shift in the critical coupling, in the form $\beta_c = \beta_c^{\text{pure}} - \Delta\beta_F$, was found to hold rather well down to small values of the fermion mass. It is convenient to work with a hopping parameter κ defined by $\kappa = \frac{1}{2m_F}$, where m_F is the fermion mass. As shown in Fig. 1, the Hasenfratz-DeGrand results for $N_t = 4$ are in excellent agreement out to at least $\kappa = 2$, and in reasonable agreement at $\kappa = 5$; this is particularly surprising since $\Delta\beta_F$ is calculated using lattice perturbation theory at zero temperature. In order to understand the effects of finite temperature, we have calculated the one-loop fermionic corrections to the spatial and temporal plaquette couplings, as well as the leading Z_N symmetry breaking coupling.

II. RENORMALIZATION OF β AT FINITE TEMPERATURE

A. Perturbation Theory for $\Delta\beta$

The $O(A^2)$ term in the gauge field lattice action including the one-loop finite temperature fermionic correction is given by

$$S_{\text{eff}} = -g^2 \sum_{p_0} \frac{1}{N_t} \int_{-\pi}^{\pi} \frac{d^3\vec{p}}{(2\pi)^3} \text{Tr}_c \left\{ \tilde{A}_\mu(p) \tilde{A}_\nu(p) \frac{\beta}{2N_c} [D_{\mu\nu}^{(0)}(p) + D_{\mu\nu}^{(1)}(p) - D_{\mu\nu}^{(2)}] \right\} \quad (2.1)$$

where

$$D_{\mu\nu}^{(0)}(p) = 4 \left[\delta_{\mu\nu} \sum_{\alpha} \sin^2\left(\frac{p_\alpha}{2}\right) - \sin\left(\frac{p_\mu}{2}\right) \sin\left(\frac{p_\nu}{2}\right) \right], \quad (2.2)$$

$$D_{\mu\nu}^{(1)}(p) = \frac{1}{2} \sum_{k_0} \frac{1}{N_t} \int_{-\pi}^{\pi} \frac{d^3(\vec{k})}{(2\pi)^3} \text{Tr}_d \left[R(k_\mu + \frac{p_\mu}{2}) S^{-1}(k) R(k_\nu + \frac{p_\nu}{2}) S^{-1}(k+p) \right], \quad (2.3)$$

and

$$D_{\mu\nu}^{(2)} = \frac{1}{2} \delta_{\mu\nu} \sum_{k_0} \frac{1}{N_t} \int_{-\pi}^{\pi} \frac{d^3(\vec{k})}{(2\pi)^3} \text{Tr}_d \left[Q(k_\mu) S^{-1}(k) \right] \quad (2.4)$$

with the vertex functions given by

$$R(k_\mu) = i\gamma_\mu \cos(k_\mu) \quad (2.5)$$

and

$$Q(k_\mu) = -i\gamma_\mu \sin(k_\mu) \quad (2.6)$$

with no sum over μ . The inverse fermion propagator is

$$S(k) = \frac{1}{2\kappa} + i\gamma_\mu \sin(k_\mu). \quad (2.7)$$

This formula is a straightforward consequence of the lattice Feynman rules, which are given in Fig. 2. The diagrams contributing to the fermionic renormalization of $\Delta\beta$ are shown in Fig. 3. The first diagram, corresponding to $D^{(0)}$, is the free lattice gluon propagator. The second diagram, corresponding to $D^{(1)}$, involves R and S only and survives in the continuum limit; note that R is the lattice analog of the continuum gluon vertex. The third diagram, corresponding to $D^{(2)}$, is a lattice tadpole diagram, and involves the vertex function Q, which is a feature only of the lattice theory. At zero temperature, this tadpole contribution vanishes after integration by parts [3]. Finite temperature enters into the calculation only through the replacement of the integration over the k_0 variable appropriate for zero temperature by the sum over Matsubara frequencies

$$k_0 = \frac{2\pi n}{T} \quad (2.8)$$

where n is integer-valued and T is the temperature.

B. Ward Identity at Finite Temperature

At finite temperature, the $D^{(2)}$ term in Eq. (2.1) is necessary in order to show that the lattice form of the Ward identity

$$\sin\left(\frac{P_\nu}{2}\right) [D_{\mu\nu}^{(2)}(p) - D_{\mu\nu}^{(1)}] = 0 \quad (2.9)$$

still holds at finite temperature, even though the four dimensional hypercubic symmetry is broken. To show this, we first note the two identities

$$S(k+p) - S(k) = 2 \sin\left(\frac{p_\mu}{2}\right) R\left(k_\mu + \frac{p_\mu}{2}\right) \quad (2.10)$$

and

$$R\left(k_\mu + \frac{p_\mu}{2}\right) - R\left(k_\mu - \frac{p_\mu}{2}\right) = 2 \sin\left(\frac{p_\mu}{2}\right) Q(k_\mu). \quad (2.11)$$

Use of the first identity gives

$$\begin{aligned} \sin\left(\frac{P_\nu}{2}\right) [D_{\mu\nu}^{(2)}(p) - D_{\mu\nu}^{(1)}] &= \frac{1}{4} \sum_k \frac{1}{N_t V} \text{Tr}_d \left\{ 2 \sin\left(\frac{p_\mu}{2}\right) Q(k_\mu) S^{-1}(k) \right. \\ &\quad \left. + \left[R\left(k_\mu + \frac{p_\mu}{2}\right) S^{-1}(k_\mu + p_\mu) - R\left(k_\mu + \frac{p_\mu}{2}\right) S^{-1}(k_\mu) \right] \right\}, \quad (2.12) \end{aligned}$$

and after a simple shift of variables, use of the second identity yields the desired cancellation.

C. Finite Temperature Decomposition of the Propagators

At finite temperature there are two independent symmetric tensors of order p^2 which are four-dimensionally transverse [4]. In what follows, all expressions will be in the thermal rest frame. The first of the corresponding lattice tensors is specified by

$$P_{\mu 0}^{(3)}(p) = P_{0\mu}^{(3)}(p) = 0 \quad (2.13)$$

$$P_{ij}^{(3)}(p) = \delta_{ij} - \frac{\tilde{p}_i \tilde{p}_j}{\tilde{p}_s^2} \quad (2.14)$$

and the second is

$$P_{\mu\nu}^{(4)}(p) - P_{\mu\nu}^{(3)}(p) \quad (2.15)$$

where

$$P_{\mu\nu}^{(4)}(p) = \delta_{\mu\nu} - \frac{\tilde{p}_\mu \tilde{p}_\nu}{\tilde{p}^2} \quad (2.16)$$

The lattice quantities \tilde{p} are defined by

$$\tilde{p}_\mu = 2 \sin\left(\frac{p_\mu}{2}\right) \quad (2.17)$$

$$\tilde{p}^2 = \sum_{\mu} \tilde{p}_\mu^2 \quad (2.18)$$

$$\tilde{p}_s^2 = \sum_i \tilde{p}_i^2 \quad (2.19)$$

The existence of these two independent tensors leads to separate renormalizations of the spatial and temporal gauge couplings at finite temperature. The first tensor, $P_{\mu\nu}^{(3)}(p)$, is associated with the magnetic, or spatial, part of the action, while the second tensor, $P_{\mu\nu}^{(4)}(p) - P_{\mu\nu}^{(3)}(p)$, is associated with the electric, or temporal, part of the action.

We find that

$$\Delta\beta_s = -N_c \sum_{k_0} \frac{1}{N_t} \int_{-\pi}^{\pi} \frac{d^3 \vec{k}}{(2\pi)^3} \Phi(k; 1, 2) \quad (2.20)$$

and

$$\Delta\beta_t = -N_c \sum_{k_0} \frac{1}{N_t} \int_{-\pi}^{\pi} \frac{d^3 \vec{k}}{(2\pi)^3} \Phi(k; 0, 1) \quad (2.21)$$

where

$$\begin{aligned} \Phi(k; \mu, \nu) &= 32B^{-2}(k) \cos^2(k_\mu) \cos^2(k_\nu) \\ &\quad - 4096B^{-4}(k) \sin^2(k_\mu) \cos^2(k_\mu) \sin^2(k_\nu) \cos^2(k_\nu) \end{aligned} \quad (2.22)$$

and

$$B(k) = \frac{1}{\kappa^2} + 4 \sum_{\alpha} \sin^2(k_\alpha). \quad (2.23)$$

As the temperature is taken to zero, the two expressions smoothly approach each other to give the zero-temperature result.

D. Numerical Results for $\Delta\beta$

The integrals (2.20) and (2.21) were evaluated numerically by calculating mode sums for large values of N_s and various values of N_t . Figure 4 compares $\Delta\beta$ per fermion (spatial and temporal) vs. κ for $N_t = 4$ and $N_t = 6$ with the zero temperature result of Hasenfratz and DeGrand [1]. The finite temperature values approach the zero temperature result from below as a consequence of the antiperiodic boundary conditions; as N_t increases, the sum includes more terms in the region near $p = 0$, which dominates for small m_F . As might be expected, the temporal shift in β is more sensitive to the effect of finite temperature than the spatial shift. For small values of κ , corresponding to large values of the fermion mass, the effects of finite temperature are small. This is easily understood, since κ is much smaller than N_t . However, for intermediate values of κ , finite temperature corrections ruin the excellent agreement between the zero-temperature calculation and the Monte Carlo results discussed in Sec. I.

E. Image Expansion

The connection between the the zero and finite temperature result can be understood more physically by transforming the sum over Matsubara frequencies into a sum over images using the Poisson summation formula for antiperiodic boundary conditions

$$\sum_{p_0} \frac{1}{N_t} F(p_0) = \sum_n (-1)^n \int_{-\pi}^{\pi} \frac{dp_0}{2\pi} F(p_0) e^{inN_t p_0} \quad (2.24)$$

so that, for example, the shift in the spatial coupling is given by

$$\Delta\beta_s = -N_c \int_{-\pi}^{\pi} \frac{d^4k}{(2\pi)^4} \Phi(k; 1, 2) - 2N_c \sum_{n=1}^{\infty} (-1)^n \int_{-\pi}^{\pi} \frac{d^4k}{(2\pi)^4} \Phi(k; 1, 2) \cos(nN_t k_0) \quad (2.25)$$

with a similar result for $\Delta\beta_t$. This form has a simple physical interpretation: the first integral is the zero-temperature shift, and the integer n in the second term labels the net number of times the fermion wraps around the lattice in the temporal direction. The finite temperature corrections result from the $O(A^2)$ expansion of image diagrams such as those

depicted in Fig. 5. Numerically, the dominant corrections to the zero-temperature result come from the first few values of n , with the $n = 1$ and $n = 2$ terms accounting for more than 90% of the finite temperature correction for $\kappa \leq 2.0$.

Although not apparent in our perturbative calculations, in order to maintain gauge invariance, the vertical segments of the image diagrams must be accompanied by powers of Polyakov loops. It is an observed feature of simulations with dynamical fermions that the Z_N symmetry is approximately maintained in the low-temperature phase. This suggests that the image contributions may be negligible below β_c . Thus, the zero temperature corrections to β are suppressed nonperturbatively in the confined regime. In particular, just below β_c the zero-temperature result will hold for $\Delta\beta$. Figure 6 illustrates an idealized behaviour for $\Delta\beta_{\text{fermion}}$ as a function of β_{pure} .

III. Z_N SYMMETRY BREAKING IN THE EFFECTIVE ACTION

There is another set of terms induced by the fermion determinant only at finite temperature. As is well known, the Z_N symmetry of the pure gauge theory is explicitly broken by dynamical fermions. To lowest order in the hopping parameter expansion, a path of N_t hops around the lattice in the temporal direction produces a effective coupling to the Polyakov loop, explicitly breaking the Z_N symmetry. Evaluating the fermion determinant in a constant A_0 background field and applying the Poisson summation formula [Eq. (2.24)] once again, we find an additional contribution to the effective action:

$$S_{\text{eff}} = \sum_{\vec{x}} \sum_{n=1}^{\infty} (-1)^{n+1} h_n(\kappa) \text{Re} \left[\text{Tr} P^n(\vec{x}) \right] \quad (3.1)$$

where $P(\vec{x})$ denotes a Polyakov loop and the couplings h_n are given by

$$h_n(\kappa) = -4N_t \int_{-\pi}^{\pi} \frac{d^4q}{(2\pi)^4} \ln \left[\frac{1}{4\kappa^2} + \sum_{\mu} \sin^2(q_{\mu}) \right] \cos(nN_t q_0) \quad (3.2)$$

This result can also be obtained by using a contour integral to evaluate the sum over Matsubara frequencies. The leading term in this effective action has been discussed for the case $N_t = 2$ [5].

A. Numerical Results for h

The maximum values of the h_n are obtained when $m_F = 0$. For $N_t = 4$ we find $h_1^{\max} = 0.107$, $h_2^{\max} = 0.00445$, and increasingly smaller magnitudes for higher order couplings. Because h_1 favors Z_N breaking, it acts to lower the critical value of β . Unlike the $D^{(1)}(p)$ term considered in Sec. II, this effect cannot be directly included as a finite shift in β . The most direct way to determine the shift in β due to h_1 term is to perform a Monte Carlo simulation of the pure gauge theory with an h_1 term added to the action. The numerical simulation results presented in this section were obtained from runs of 40,000 sweeps (after thermalization) on a $10^3 \times 4$ lattice using a variety of work stations.

We have observed that this additional source of $\Delta\beta$ is small compared to the renormalization of the plaquette couplings discussed in the preceding section, regardless of m_F . For example, even $h_1 = 0.1$ at $N_t = 4$ leads to a shift in β per fermion of 0.00325. This value of h_1 corresponds to $m_F = 0.17$ which yields a zero-temperature predicted shift in β per fermion of 0.104. Although the effect of the h_1 term in the effective action on the critical value of β is quite small, h_1 has a profound effect on the character of the transition. Figure 7 shows the frequency distribution for the spatial expectation value of the Polyakov loop as a function of h_1 at the appropriate $\beta_c(h_1)$ on a $10^3 \times 4$ lattice. As h_1 increases, the peaks associated with the two phases move closer together until they merge at what is presumably a second-order critical end-point. A first-order phase transition exists for values of h_1 smaller than approximately 0.08.

The Monte Carlo results for the phase diagram of a pure gauge theory with an h_1 coupling can be mapped back to the phase diagram of QCD with dynamical quarks by including both the h_1 term and the shift $\Delta\beta$. Including zero-temperature plaquette coupling renormalization, the endpoint of this first-order phase transition line maps to the point (0.394, 4.68) in the (m_F, β) -plane for the case of sixteen degenerate staggered fermion species. This is roughly consistent with the endpoint of the first-order phase transition observed in simulations with dynamical staggered fermions [6]. However, a definitive comparison will

likely require significant computational resources.

IV. CONCLUSIONS

Figure 8, a graph of β_c versus κ , summarizes the results we have obtained. As shown by Hasenfratz and DeGrand, the zero-temperature shift in the coupling constant due to dynamical fermions nicely accounts for the shift in β_c . We have found that finite temperature corrections to the gauge coupling renormalization lift the degeneracy of the spatial and temporal couplings, and the results are significantly different from the zero-temperature results. As can be seen from the figure, they are in conflict with the Monte Carlo data. At finite temperature, dynamical fermions couple to Polyakov loops via loops circling the lattice in the timelike direction. This also acts to shift the value of β_c . This shift is small, however, and does not restore the success of the zero-temperature calculation.

As we have shown, the image expansion makes it plausible that the success of the zero-temperature calculation in determining the critical value of β is due to a nonperturbative suppression of finite temperature effects in the low temperature regime. Specifically, the small expectation value of the Polyakov loops at low temperatures indicates a suppression of those quark paths which account for finite temperature corrections. This leads to the behavior of the effective gauge coupling constants shown in Fig. 5 above. If this picture is correct, a gauge theory with dynamical fermions of intermediate mass is well modeled by a pure gauge theory in which the spatial and temporal couplings are slightly different. Along the critical line, both couplings jump discontinuously. This could be studied in more detail by adjusting spatial and temporal couplings in a pure gauge theory simulation so that plaquette expectation values matched those observed in dynamical simulations. This might also afford an opportunity to consider the effects of finite spatial sizes. Such effects are easily included in Eq. 2.25 for the coupling shift by choosing the spatial mode sums appropriately.

While the coupling to Polyakov loops induced by dynamic fermion loops seems to play little role in determining β_c , this coupling does influence the order of the transition; in our

$N_t = 4$ simulations of a pure gauge theory with an additional coupling h_1 to Polyakov loops, a sufficiently large value of h_1 causes the first order line to terminate, while shifting β_c very little. Thus, the effective coupling h_1 appears to be the most important factor in determining the end point of the first-order deconfining phase transition line.

In addition to the transition temperature, other quantities can be estimated using these perturbative techniques. For example, the chiral order parameter $\langle \bar{\psi}\psi \rangle$ can be estimated as a constant term plus a term proportional to the expectation value of a plaquette plus a term proportional to the expectation value of the Polyakov loop. However, the use of a perturbative evaluation of the fermion determinant obviously fails to include the effects of chiral symmetry breaking, which is the dominant factor in determining $\langle \bar{\psi}\psi \rangle$ for light quarks. Presumably this accounts for the failure of the effective theory for light quark masses.

V. ACKNOWLEDGEMENTS

We would like to thank the U.S. Department of Energy for financial support under Contract No. DE-AC02-76-CH00016. One of us (PNM) would also like to thank the U.S. Department of Education for additional financial support in the form of a GANN Predoctoral Fellowship.

REFERENCES

- [1] A. Hasenfratz and T. DeGrand, Phys. Rev. D **49**, 466 (1994).
- [2] A. Hasenfratz and T. DeGrand, Nucl. Phys. B (Proc. Suppl.) **34**, 317 (1994).
- [3] W. Celmaster and D. Maloof, Phys. Rev. D **24**, 2730 (1981).
- [4] K. Kajantie and J. Kapusta, Ann. Phys. **160**, 477 (1985).
- [5] P. Hasenfratz, F. Karsch, and I. O. Stamatescu, Phys. Lett. **133B**, 221 (1983).
- [6] S. Ohta and S. Kim, Phys. Rev. D **44**, 504 (1991).

FIGURES

FIG. 1. Predicted values (circles) of $\Delta\beta$ per fermion at zero temperature versus κ compared with finite temperature simulation results (squares).

FIG. 2. Lattice Feynman rules to $\mathcal{O}(A^2)$. The Q vertex is not present in the continuum limit.

FIG. 3. One-loop diagrams contributing to the fermionic renormalization of $\Delta\beta$.

FIG. 4. Spatial and temporal values of $\Delta\beta$ per fermion versus κ for $N_t = 4, 6, \text{ and } \infty$.

FIG. 5. Typical diagrams from the expansion of $\Delta\beta$ in images.

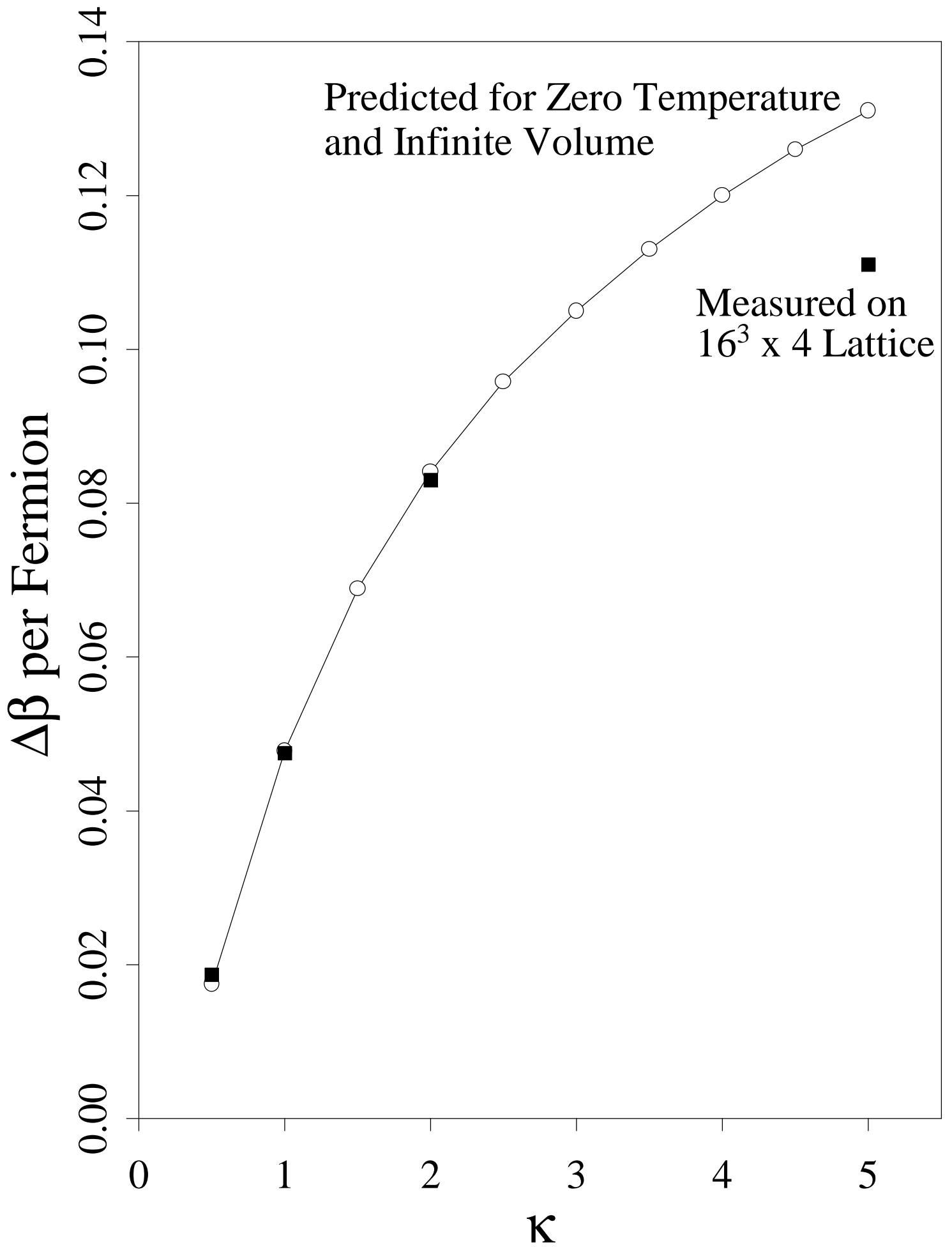
FIG. 6. Idealized behaviour of $\Delta\beta_{\text{fermion}}$ as a function of β_{pure} .

FIG. 7. Frequency distribution for the expectation value of the Polyakov loop on a $10^3 \times 4$ lattice at $\beta_c(h_1)$ for $h_1 = 0.025, 0.05, 0.075, \text{ and } 0.1$.

FIG. 8. $\Delta\beta$ per fermion versus κ computed at zero temperature, at finite temperature, and at finite temperature with a correction for Polyakov loop effects compared with finite temperature simulation results.

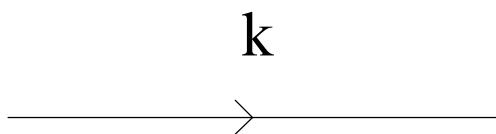
This figure "fig1-1.png" is available in "png" format from:

<http://arxiv.org/ps/hep-lat/9502003v1>

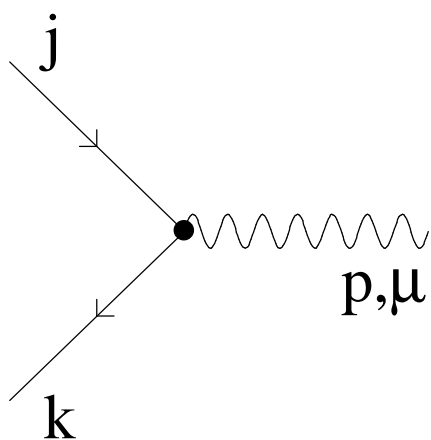


This figure "fig1-2.png" is available in "png" format from:

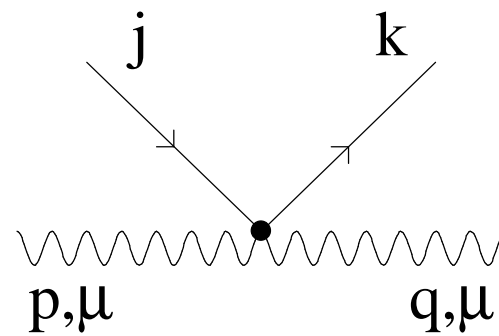
<http://arxiv.org/ps/hep-lat/9502003v1>



$$S^{-1}(k)$$



$$R(j_{\mu}/2 + k_{\mu}/2)$$



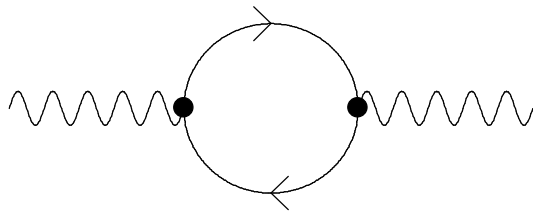
$$Q(j_{\mu}/2 + k_{\mu}/2)$$

This figure "fig1-3.png" is available in "png" format from:

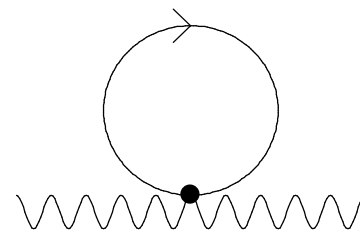
<http://arxiv.org/ps/hep-lat/9502003v1>



$D^{(0)}(\mathbf{p})$



$D^{(1)}(\mathbf{p})$

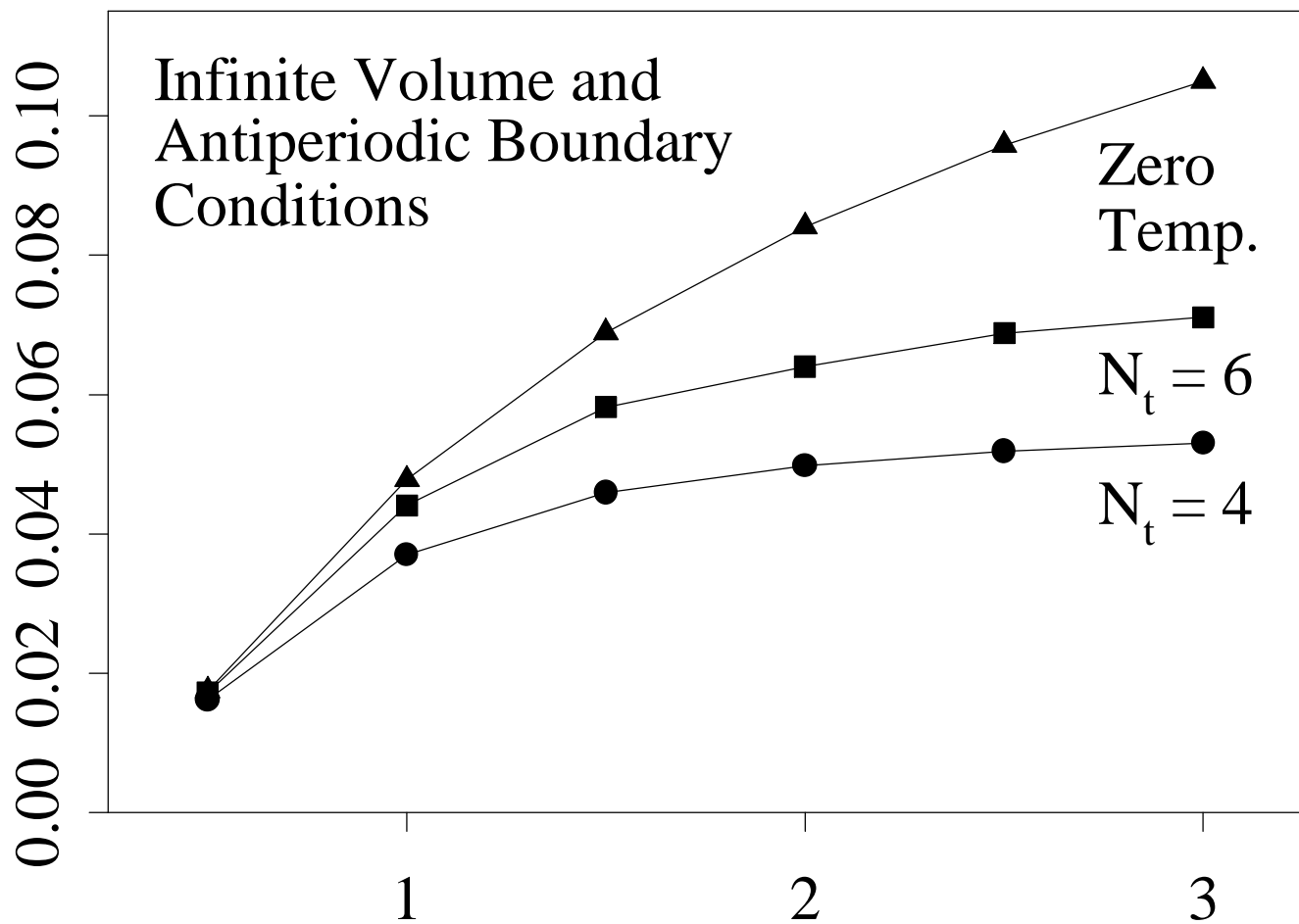


$D^{(2)}$

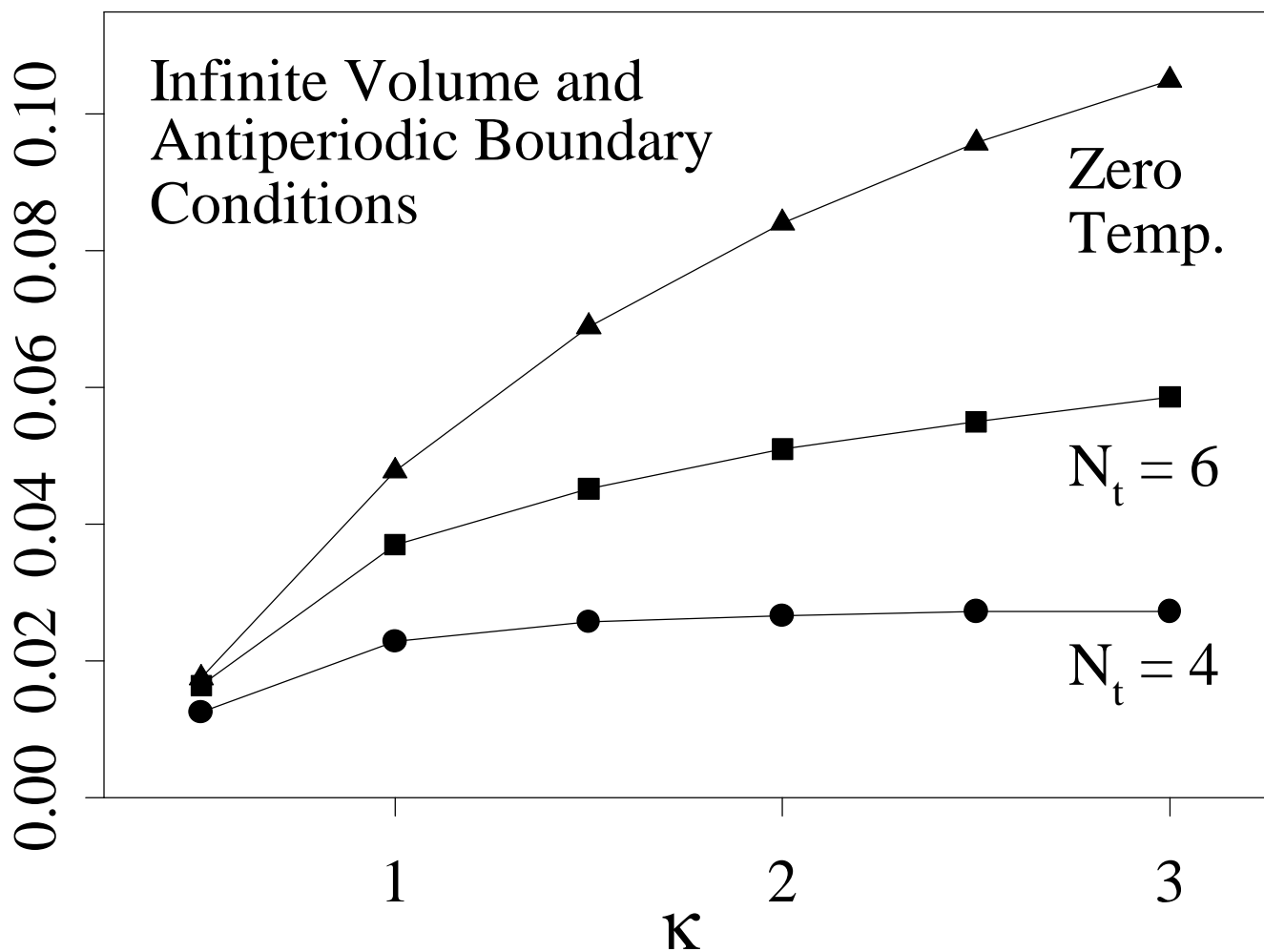
This figure "fig1-4.png" is available in "png" format from:

<http://arxiv.org/ps/hep-lat/9502003v1>

$\Delta\beta$ per Fermion (Spatial)

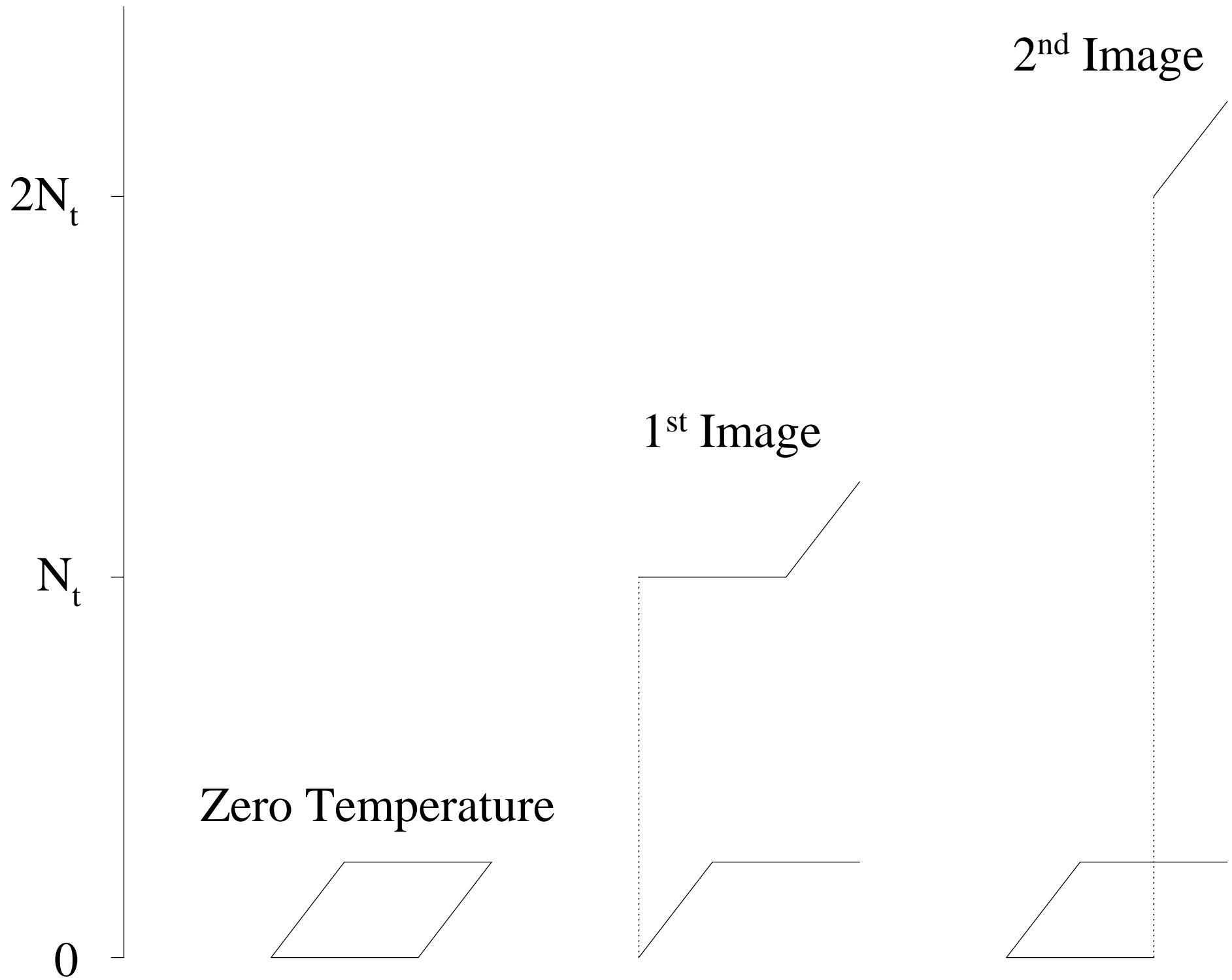


$\Delta\beta$ per Fermion (Temporal)



This figure "fig1-5.png" is available in "png" format from:

<http://arxiv.org/ps/hep-lat/9502003v1>



This figure "fig1-6.png" is available in "png" format from:

<http://arxiv.org/ps/hep-lat/9502003v1>

$\Delta\beta_{\text{fermion}}$

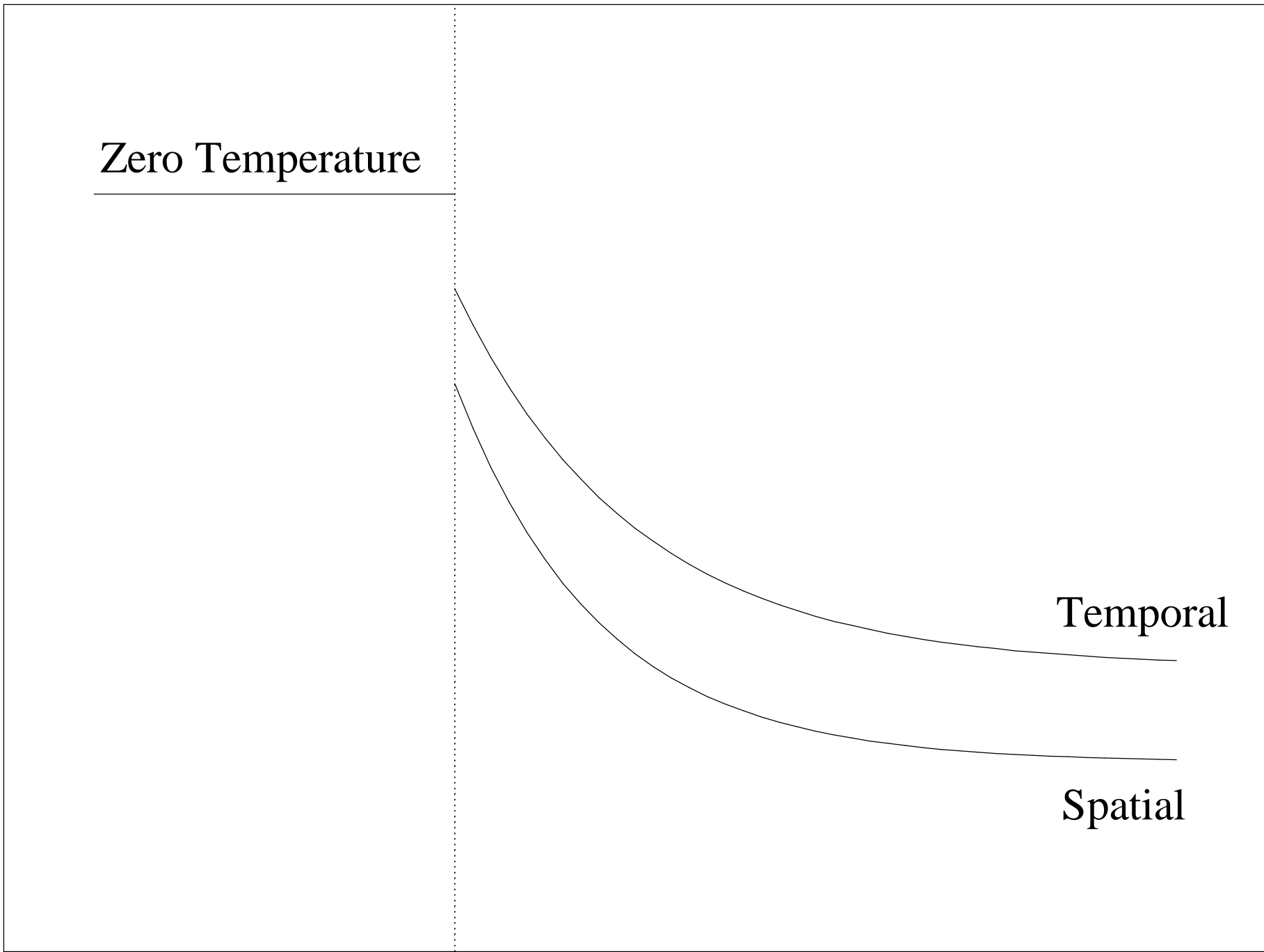
Zero Temperature

Temporal

Spatial

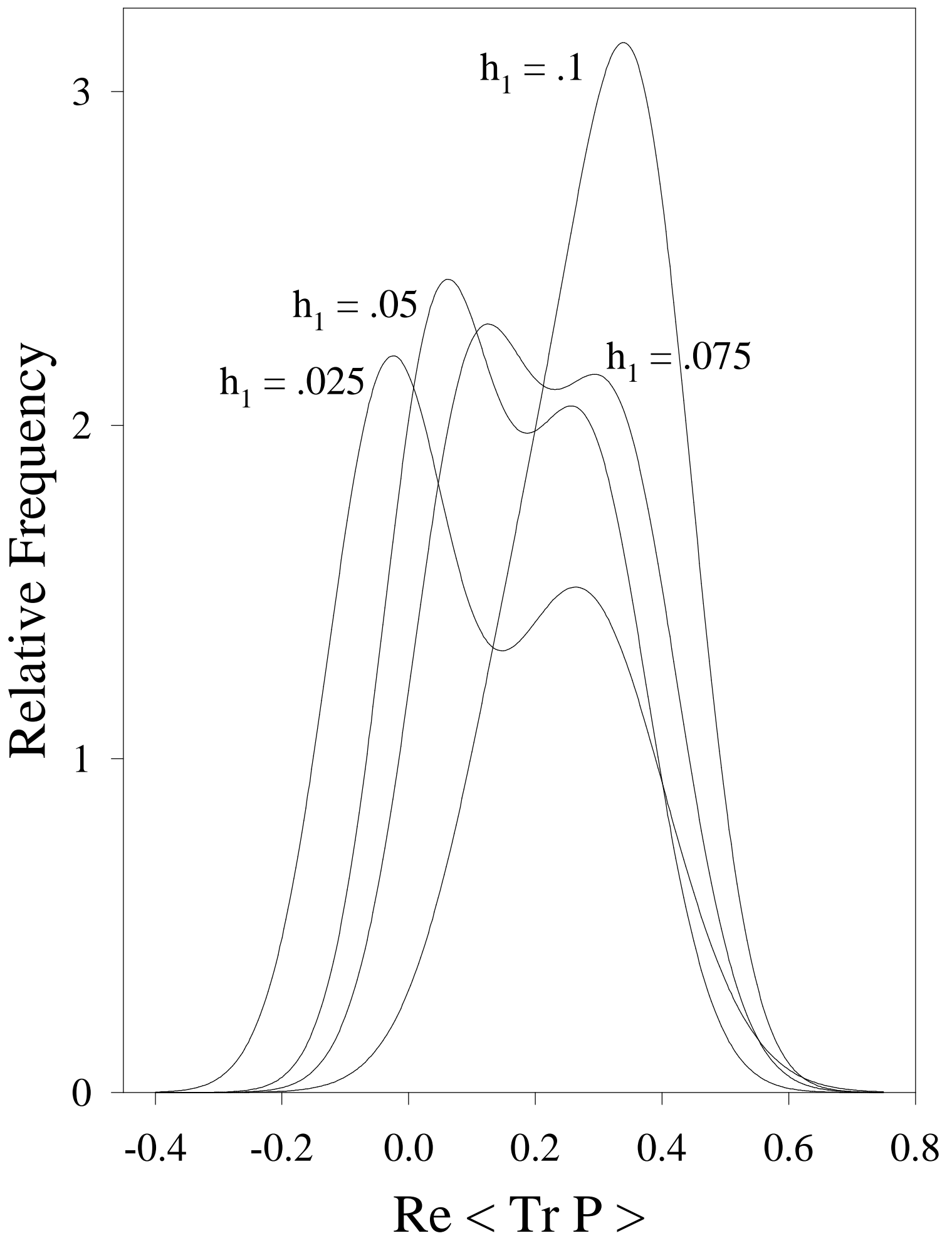
β_c

β_{bare}



This figure "fig1-7.png" is available in "png" format from:

<http://arxiv.org/ps/hep-lat/9502003v1>



This figure "fig1-8.png" is available in "png" format from:

<http://arxiv.org/ps/hep-lat/9502003v1>

